DEBYE-HÜCKEL, THOMAS-FERMI THEORY OF PLASMAS AND LIQUID METALS: NUMERICAL SOLUTION*

Robert D. Cowan

University of California
Los Alamos Scientific Laboratory
Los Alamos, New Mexico

and

John G. Kirkwood

Sterling Chemistry Laboratory
Yale University
New Haven, Connecticut

ABSTRACT

A Debye-Hückel-type theory is described for an assembly of completely ionized atoms, the nuclei being treated classically and the electrons by the Thomas-Fermi method. The thermodynamic functions are derived by considering the Debye charging process, and the virial theorem is shown to hold. Numerical results are given for hydrogen and iron near normal solid densities, and are probably accurate only at high temperatures ($kT > 5$ ev for hydrogen and $kT > 100$ ev for iron).

*Work performed under the auspices of the U. S. Atomic Energy Commission.

DISCLAIMER

1. INTRODUCTION

The temperature-dependent Thomas-Fermi (TF)[1] and Thomas-Fermi-Dirac (TFD)[2] theories of the atom have been recently discussed in detail, and used to calculate equations of state of the elements at high temperatures and pressures. These theories involve a number of approximations, among which are the following: (1) The properties of bulk material are approximated by those of an isolated, spherically-symmetric atom whose nucleus is at rest. There are thus no contributions due to nuclear motion nor to interactions between neighboring atoms. (2) The electrons are assumed to be quasi-free, and their distribution about the nucleus is calculated statistically, so that the shell structure of the atom is in no way reproduced. The electron density at the nucleus turns out to be infinite, resulting in absolute binding energies which are considerably too great in magnitude. (3) The electrons are treated in the one-electron approximation, so that there are no correlations in the motions of the electrons due to their mutual electrostatic repulsion, though in the TFD theory, some correlation among electrons of parallel spin results from effects of the Pauli exclusion principle.

The Debye-Hückel, Thomas-Fermi (DHTF) theory developed recently by Plock and Kirkwood[3] removes to some extent several of the above approximations. Matter is treated in bulk with associated nuclear effects and interactions between atoms, and electrostatic correlations among the electrons are present. Exchange effects are not included. These can be incorporated in a manner similar to that of the TFD theory (the principle change in the equations given below is to replace $\frac{1}{2}\theta^{3/2}I_{1/2}(\eta)$ by the function $G_2(\theta\eta,\theta)$ defined in reference 2); however, this would introduce fairly serious numerical complications and would probably not greatly change the calculated

results since at low densities, the correlation effects include most or all of the exchange energy.[4]

2. THEORY

We consider an infinite assembly of atoms (of one element) at uniform temperature and density, such that all particles (both nuclei and electrons) are free to move about under the influence of their mutual electrostatic forces. In order to be able to evaluate the thermodynamic functions for this system by considering the Debye charging process, we suppose each particle to carry an arbitrary fraction λ of its true physical charge, the charge on each particle thus being λZe and $-\lambda e$ for nuclei and electrons, respectively. The average densities of nuclei and electrons will be denoted by n_{+o} and n_{-o}; for an electrically neutral system

$$Zn_{+o} = n_{-o}. \tag{1}$$

A. Particle Distributions About a Nucleus

Singling out one particular nucleus, let the average electrostatic potential (due to all particles, including the nucleus in question) and the average charge density about this nucleus be respectively $\psi_+(r)$ and

$$\rho_+(r) = \lambda Zen_{++}(r) - \lambda en_{-+}(r), \tag{2}$$

where n_{++} and n_{-+} are the average densities of nuclei and electrons at a distance r from the given nucleus. The potential and charge density are

related through the Poisson equation

$$\Delta\psi_+ = -4\pi\rho_+ = -4\pi\lambda e(Zn_{++} - n_{-+}), \tag{3}$$

the boundary conditions being

$$\begin{aligned} &\lim_{r\to o} r\psi_+(r) = \lambda Ze \\ &\lim_{r\to\infty} \psi_+(r) = 0. \end{aligned} \tag{4}$$

We shall assume that the nuclei can be treated classically, so that

$$n_{++} = n_{+o}\, e^{-\lambda Ze\psi_+/kT}. \tag{5}$$

The electrons must, however, be described by Fermi-Dirac statistics. In the Thomas-Fermi approximation, we have[5]

$$\begin{aligned} n_{-+} &= \frac{8\pi}{h^3} \int_o^\infty \frac{p^2 dp}{1 + \exp\left[(p^2/2m - \lambda e\psi_+ - \mu)/kT\right]} \\ &= 4\pi(2mkTh^{-2})^{3/2} I_{1/2}(\eta_+), \end{aligned} \tag{6}$$

where

$$I_m(\eta) = \int_o^\infty y^m\, (1 + e^{y-\eta})^{-1}\, dy, \tag{7}$$

$$\eta_+ = (\lambda e\psi_+ + \mu)/kT, \tag{8}$$

and the free-electron chemical potential μ is such that

$$n_{-o} = 4\pi(2mkTh^{-2})^{3/2} I_{1/2}(\eta_\infty), \tag{9}$$

$$\eta_\infty = \mu/kT. \tag{10}$$

For purposes of numerical calculation, it is convenient to introduce the following units of length and energy[6]

$$r_\lambda = \frac{h^2}{4\pi^2 m\lambda^2 e^2}\left(\frac{9\pi^2}{128Z}\right)^{1/3} = \frac{0.468479\cdot 10^{-8}}{\lambda^2 Z^{1/3}} \text{ cm}, \tag{11}$$

and

$$\theta_\lambda = 32m\lambda^4 e^4 h^{-2} = 22.0532\,\lambda^4 \text{ ev}, \tag{12}$$

and also the quantities

$$x = r/r_\lambda, \qquad \theta = kT/\theta_\lambda, \tag{13}$$

$$4\epsilon = (6/\pi^2 Z^2)^{1/3} = 0.84713084\, Z^{-2/3}, \tag{14}$$

$$\eta_+ = \theta^{-1}(4\epsilon)^{-2}(\phi_+/x). \tag{15}$$

Combining all the above, the Poisson equation (3) reduces to

$$\phi''_+(x) = \frac{3}{2}(4\epsilon)^3\theta^{3/2}x\left[I_{1/2}(\eta_+) - I_{1/2}(\eta_\infty)e^{-Z(\eta_+-\eta_\infty)}\right], \tag{16}$$

with boundary conditions

$$\phi_+(o) = 1,$$
$$\lim_{x\to\infty}\phi_+(x) = x(\phi/x)_\infty = x\phi'_\infty. \tag{17}$$

For given temperature, bulk density of material, and value of λ, the procedure is as follows: n_{-o} can be readily calculated from the bulk density, θ found from (13), $I_{1/2}(\eta_\infty)$ from (9), and η_∞ from the tables and asymptotic expansions for $I_{1/2}$ given by McDougall and Stoner.[7] The differential equation (16) can then be integrated to give $\phi_+(x)$, and hence $\eta_+(x)$ from (15). The distribution of particles about a given nucleus then follows from (6) and the equivalent of (5)

$$n_{++} = n_{+o}\, e^{-Z(\eta_+-\eta_\infty)}. \tag{18}$$

The net charge surrounding the given nucleus is

$$q_+ = 4\pi\, r_\lambda^3 \int_o^\infty (\lambda Z e n_{++} - \lambda e n_{-+})x^2 dx. \tag{19}$$

Using (6), (18), and the differential equation (16), this can be written

$$q_+ = -\lambda Ze \int_0^\infty \phi_+'' x dx$$

$$= -\lambda Ze \left[x\phi_+' - \phi_+ \right]_0^\infty = -\lambda Ze, \tag{20}$$

from the boundary conditions (17). Thus q_+ is, as it should be, the negative of the charge on the given nucleus.

B. Particle Distributions About an Electron

Singling out a specific electron, let the average electrostatic potential (due to all charges, including the electron in question) and the average charge density about this electron be respectively $\psi_-(r)$ and

$$\rho_-(r) = \lambda Z e n_{+-}(r) - \lambda e n_{--}(r). \tag{21}$$

These quantities are related through the Poisson equation

$$\Delta\psi_- = -4\pi\rho_- = -4\pi\lambda e(Zn_{+-} - n_{--}), \tag{22}$$

with boundary conditions

$$\lim_{r\to 0} r\psi_-(r) = -\lambda e$$

$$\lim_{r\to\infty} \psi_-(r) = 0. \tag{23}$$

For a neutral plasma, it follows from symmetry considerations that the distribution of positive charge about an electron must be identical in form to the distribution of negative charge about a nucleus. Thus from (6),

$$n_{+-} = Z^{-1}n_{-+} = 4\pi Z^{-1}(2mkTh^{-2})^{3/2} I_{1/2}(\eta_+). \tag{24}$$

Letting

$$\eta_- = (\lambda e\psi_- + \mu)/kT = \lambda e\psi_-/kT + \eta_\infty , \tag{25}$$

then analogously to (6)

$$n_{--} = 4\pi(2mkTh^{-2})^{3/2} I_{1/2}(\eta_-). \tag{26}$$

Introducing a function $\phi_-(x)$ defined by

$$\eta_- = \theta^{-1}(4\epsilon)^{-2}(\phi_-/x), \tag{27}$$

the Poisson equation (22) becomes

$$\phi_-''(x) = \tfrac{3}{2}(4\epsilon)^3\theta^{3/2}x\left[I_{1/2}(\eta_-) - I_{1/2}(\eta_+)\right], \tag{28}$$

with boundary conditions

$$\phi_-(o) = -1/Z,$$

$$\lim_{x\to\infty} \phi_-(x) = x(\phi/x)_\infty = x\,\phi'_\infty . \tag{29}$$

With $I_{1/2}(\eta_+)$ being a known function of x from the solution of (16), (28) can readily be integrated to give ϕ_- and η_- as functions of x, thereby giving the distribution of particles about an electron from (24) and (26).

Similarly to the derivation of (20), the net charge about a given electron is

$$q_- = 4\pi r_\lambda^3 \int_o^\infty (\lambda Z e n_{+-} - \lambda e n_{--}) x^2 dx$$

$$= -\lambda Z e \left[x\phi'_- - \phi_- \right]_o^\infty = \lambda e, \tag{30}$$

which is just the negative of the charge on the electron.

C. The Thermodynamic Functions

An expression for the Helmholtz free energy A(v,T) of our system will be derived through the artifice of the Debye charging process, and we accordingly write

$$A = A_i + A_e, \tag{31}$$

where A_i is the Helmholtz free energy of the uncharged (ideal) plasma, and A_e is the contribution which arises during the charging process.

The contribution of the nuclei to the ideal Helmholtz energy A_i (per atom) is given by the classical expression

$$A_{i+} = -kT \left\{1 + \ln \left[(2\pi m_+ kT)^{3/2}/h^3 n_{+o} \right]\right\} , \tag{32}$$

and the contribution of the electrons (per atom) is[8]

$$A_{i-} = ZkT \left\{\eta_\infty - \frac{2}{3} I_{3/2}(\eta_\infty)/I_{1/2}(\eta_\infty)\right\} . \tag{33}$$

The portion A_e of the Helmholtz energy is the electrical work done in charging up the particles at constant temperature and volume, the particle distributions at each stage in the charging process being the equilibrium distributions for the corresponding value of λ. Thus the contribution of each nucleus to A_e is

$$A_{e+} = \int_o^{Ze} \lim_{r\to o} \left[\psi_+(r,\lambda) - \frac{\lambda Ze}{r} \right] d(\lambda Ze)$$

$$= \frac{Ze^2}{a_o} \left(\frac{4Z^2}{3\pi}\right)^{2/3} \int_o^1 \lambda^2 \left[\phi_+'(o) - \left(\frac{\phi}{x_\infty}\right)\right]_\lambda d(\lambda^2), \tag{34}$$

and the contribution of Z electrons to A_e is

$$A_{e-} = Z \int_o^{-e} \lim_{r\to o} \left[\psi_-(r,\lambda) + \frac{\lambda e}{r}\right] d(-\lambda e)$$

$$= -\frac{Ze^2}{a_o} \left(\frac{4Z^2}{3\pi}\right)^{2/3} \int_o^1 \lambda^2 \left[\phi_-'(o) - \left(\frac{\phi}{x}\right)_\infty\right]_\lambda d(\lambda^2), \tag{35}$$

where the quantities $\lambda Ze/r$ and $-\lambda e/r$ have been subtracted from ψ_+ and ψ_-, respectively, in order to remove the self-energies of the particles, and where $\phi_{\pm}(x)$ have been expanded in Taylor series about the origin (see Section 3), and the boundary conditions (17) and (29) employed. ($a_o = \hbar^2/me^2$ is the first Bohr radius of hydrogen.)

With the Helmholtz free energy calculated in this manner, the pressure and the internal energy per atom can then be obtained from the general relations

$$p = -(\partial A/\partial v)_T,$$

$$S = -(\partial A/\partial T)_v, \tag{36}$$

$$E = A + TS.$$

Alternatively, the pressure or the energy can be found from (36) and the other quantity found from the virial theorem,[9] which for Coulombic forces, has the form

$$pv = \frac{2}{3} E_k + \frac{1}{3} E_p, \tag{37}$$

where E_k and E_p are respectively the kinetic and potential energies of the system. The validity of the virial theorem in the case under consideration can be established as follows:

The energy of the uncharged gas obtained from (32), (33), and (36) is entirely kinetic, and it can be readily shown that $p_i v = \frac{2}{3} E_i$ -- using in the case of A_{i-} the relation (9)

$$vT^{3/2} I_{1/2}(\eta_\infty) = \text{constant}, \tag{38}$$

and also the relation[7] $dI_{3/2}/d\eta_\infty = \frac{3}{2} I_{1/2}$. Thus it is necessary to consider only the contribution of A_e to the pressure (p_e) and the energy (E_e). This last quantity includes not only potential energy but also a change in the kinetic energy brought about by the charging process -- the potential energy of the fully charged system being the result given by (34) and (35) if the particle distributions are held fixed at their values for $\lambda = 1$:[10]

$$E_p = \frac{Ze^2}{a_o} \left(\frac{4Z^2}{3\pi}\right)^{2/3} \left[\phi_+'(o) - \phi_-'(o)\right]_{\lambda=1} \int_o^1 d(\lambda^2). \tag{39}$$

We first note from (15)-(17) and (27)-(29) that (for given Z) the solutions $\phi_+(x)$ and $\phi_-(x)$ do not depend on v, T, and λ independently, but only on the two quantities η_∞ and Θ -- or from (38) and (13), only on

$$vT^{3/2} \text{ and } T\lambda^{-4}. \tag{40}$$

Thus if v_1 and T_1 are some fixed volume (per atom) and temperature and if v and T are quantities related to v_1 and T_1 through a scale factor c such that

$$v = c^6 v_1 \text{ and } T = c^{-4} T_1, \tag{41}$$

then A_e may be written

$$A_e(v,T) = K\int_0^1 \lambda^2 \left[\phi_+'(o) - \phi_-'(o)\right]_{v,T,\lambda} d(\lambda^2)$$

$$= Kc^{-4}\int_0^{c^2} (c\lambda)^2 \left[\phi_+'(o) - \phi_-'(o)\right]_{v_1,T_1,c\lambda} d(c^2\lambda^2),$$

where K is the constant before the integral sign in (34). Differentiation of this expression gives

$$\left(\frac{dA_e}{dc}\right)_{v_1,T_1} = -\frac{4}{c}A_e + \frac{2}{c}K\left[\phi_+'(o) - \phi_-'(o)\right]_{v_1,T_1,c}$$

$$= -\frac{4}{c}A_e + \frac{2}{c}K\left[\phi_+'(o) - \phi_-'(o)\right]_{v,T,1}. \qquad (42)$$

But from (36) and (41),

$$\left(\frac{dA_e}{dc}\right)_{v_1,T_1} = \left(\frac{A_e}{v}\right)_T \left(\frac{dv}{dc}\right)_{v_1} + \left(\frac{A_e}{T}\right)_v \left(\frac{dT}{dc}\right)_{T_1}$$

$$= -6\frac{v}{c}p_e + 4\frac{T}{c}S_e, \qquad (43)$$

and combining this with (42) and (39) gives

$$p_e v = \frac{2}{3}(A_e + TS_e) - \frac{1}{3}E_p$$

$$= \frac{2}{3}(E_e - E_p) + \frac{1}{3}E_p, \qquad (44)$$

which completes the proof of (37). (In the singular case T = 0, the proof can be carried out in a manner entirely analogous to that which has been given for a modified DHTF theory.[4])

3. NUMERICAL METHODS

The differential equations (16) and (28) were integrated numerically with the aid of IBM Type 704 digital computers, using numerical methods similar to those employed elsewhere.[2,4]

A. Integration of the Equation for ϕ_+

For small x, it may be seen from (15) and (17) that $\eta_+ \gg 1$, so that the second term in (16) is negligible compared with the first, the differential equation thus reducing to that for the temperature-dependent TF atom. The solution can, therefore, be written in series form:

$$\phi_+(x) = \sum a_i x^{i/2}, \tag{45}$$

the values of the first few coefficients being[11]

$$a_0 = 1 \quad , \quad a_1 = 0,$$

$$a_2 = \phi_+'(0) = \text{arbitrary}, \quad a_3 = 4/3$$

$$a_4 = 0 \quad , \quad a_5 = 2a_2/5,$$

$$a_6 = \frac{1}{3} \quad , \quad a_7 = 3a_2^2/70 + O(T^2).$$

For $i \geqq 7$, the a_i contain temperature-dependent terms, which however are of no importance provided (45) is used only to sufficiently small values of x.

Using an estimated value of a_2, integration of (16) was started with the aid of (45), and then continued by a difference method. Because of the boundary condition (17), at large x Eq. (16) can be written with the aid of Taylor series expansions and Eq. (15) in the form

$$\phi_+''(x) \cong K_+^2 \left[\phi_+ - x(\phi/x)_\infty \right]$$

or

$$\phi_+(x) = x(\phi/x)_\infty + Ae^{-K_+ x}, \tag{46}$$

where

$$K_+^2 = 6\epsilon\theta^{1/2} \left[dI_{1/2}(\eta)/d\eta + ZI_{1/2}(\eta) \right]_{\eta_\infty} . \tag{47}$$

At some large x, then, the constant A was evaluated so as to match (46) to the numerical solution, and the slopes of the two solutions were then compared. The value of a_2 was then modified, and an iterative procedure carried out until the two slopes were equal to the desired accuracy.

It may easily be seen that this solution of (16)-(17) is a unique one (barring solutions with singularities at finite x): For any integral of (16), the curvature is positive for $\eta_+ > \eta_\infty$, and negative for $\eta_+ < \eta_\infty$; if ϕ_1 and ϕ_2 are two integrals satisfying the boundary conditions at the origin with $\phi_1'(o) > \phi_2'(o)$, then for all x, $\phi_1(x) > \phi_2(x)$, $\phi_1'(x) > \phi_2'(x)$, and $\phi_1''(x) > \phi_2''(x)$. The solution (which satisfies both boundary conditions) has the properties $\phi_+(x) > x\phi_\infty'$, $\phi_+'(x) < \phi_\infty'$, and $\phi_+''(x) > 0$ for all x.

As a check on the integration of the differential equation, the results were used for a numerical evaluation of the integral (19); the value of q_+ thus obtained was generally equal to $-\lambda Ze$ within one-twentieth percent, except at large Z and low Θ where the function (18) changes very rapidly with x.

B. Integration of the Equation for ϕ_-

With η_+ being a known function from the solution of (16)-(17), the integration of (28) can be carried out in a similar manner. At small x, $\eta_- \ll 0$ from (27) and (29), and (28) reduces to

$$\phi_-''(x) = -\frac{3}{2}(4\epsilon)^3\Theta^{3/2}xI_{1/2}(\eta_+), \tag{48}$$

which is identical with the small-x form of (16) except for the change in sign. The solution can therefore be written

$$\phi_-(x) = \sum b_i x^{i/2}, \tag{49}$$

where

$$b_o = -1/Z,$$

$$b_1 = 0,$$

$$b_2 = \phi_-'(o) = \text{arbitrary},$$

$$b_i = -a_i,\ i \geq 3.$$

At large x, (28) can be written

$$\phi_-''(x) \cong K_-^2(\phi_- - \phi_+),$$

the solution to which is

$$\phi_-(x) = x(\phi/x)_\infty - K_-^2(K_+^2 - K_-^2)^{-1} Ae^{-K_+x} + Be^{-K_-x}, \tag{50}$$

where

$$K_-^2 = 6\epsilon\theta^{1/2}\left[\, dI_{1/2}(\eta)/d\eta \,\right]_{\eta_\infty}. \tag{51}$$

The value of b_2 is iterated on until (50) matches the numerical solution both as to value and slope at some suitably large x.

The uniqueness of the solution can again be seen from a qualitative examination of the differential equation, though the situation is somewhat more complicated than before in that two qualitatively different forms of the solution are possible: (1) $\phi_-(x) < x\phi_\infty'$, $\phi_-'(x) > \phi_\infty'$, and $\phi_-''(x) < 0$ for all x; (2) $\phi_-(x)$ not only crosses the line $x\phi_\infty'$, but also crosses the curve $\phi_+(x)$ at some point x_1 with a slope such that $\phi_+'(x_1) < \phi_-'(x_1) < \phi_\infty'$, with $\phi_-''(x) < 0$ for $x < x_1$ and $\phi_-''(x) > 0$ for $x > x_1$. For Z = 1, only the first type solution has been observed; for Z = 2, either type may occur, depending on the density and temperature; and for somewhat larger Z, only the second type has been found. The reason for this will be discussed in Section 4B.

It all cases, the numerical results checked Eq. (30) with about the same accuracy as for Eq. (19).

C. Evaluation of the Thermodynamic Functions

As pointed out earlier, the integrands of the expressions (34) and (35) for A_e can be considered as functions of only the two parameters $vT^{3/2}$ and $T\lambda^{-4}$. However, A_e was actually computed by the more time consuming but more straightforward procedure[12] of integrating the differential equations for the desired v and T and for each of twelve values of λ^2, and evaluating the λ^2 integrals with the aid of Simpson's rule.

In order to evaluate p and E, calculations were not actually done at the $v \equiv \rho^{-1}$ and T of interest but rather at $\left[(1 \pm 0.1)\rho, T \right]$ and at $\left[\rho, (1 \pm 0.1)T \right]$, and p and S calculated from (36) by numerical differentiation in a linear approximation. The associated error is roughly one percent, compared with which the errors in Simpson's rule and in integrating the differential equations are negligible.

In a few cases, the pressure was also evaluated from the virial theorem (37). In each case, the result agreed with that obtained from (36) within the one percent uncertainty in the latter.

4. RESULTS

A. Pressure

Some numerical results for the pressure are shown in Figures 1-4, which include for comparison curves showing the pressure of the uncharged ideal gas[8]

$$p_i v = -v(\partial A_i/\partial v)_T$$

$$= kT + \frac{2}{3} ZkTI_{3/2}(\eta_\infty)/I_{1/2}(\eta_\infty) \qquad (52)$$

(where v is volume per atom), and also curves showing the electronic pressure as calculated from the TF theory of the atom.[1]

It may be seen, especially from Figure 1, that at high temperatures, the value of pv/kT for the DHTF theory is greater than that for the TF theory by approximately unity, as is to be expected since the one theory includes the nuclear contribution to the pressure whereas the other does not.

At low temperatures and densities, the DHTF curves differ qualitatively from the corresponding TF curves, the former possessing distinct plateaus in Figures 3 and 4. This effect is strongly Z- (and density-) dependent, as confirmed by numerical results (not shown here) for Z = 6 and 92. It is not immediately obvious whether the large DHTF pressure calculated in the plateau region should be considered physically meaningful. One might conjecture that this reflects ionization resulting from collisions of neighboring atoms due to the thermal motion of the nuclei, which is absent in the TF picture. However, for reasons which will be discussed below, the authors feel that these large pressures may be spurious (at least in part) and that the DHTF results should not be given too much weight at low temperatures and densities.

At sufficiently low densities, the zero-temperature pressure becomes negative (Figures 1 and 4), unlike the TF theory where p becomes zero only in the limit of zero density. This is probably related to the lowering of energy due to electron correlation, which is not present in the TF theory. The DHTF pressure seems to become zero at a slightly higher density than in the TFD theory; this is reasonable since at the low electron densities at which correlation effects are important, the correlation energy in the present theory is greater than the exchange energy of the TFD theory (see reference 4 and Section 4C below).

The high-temperature regions in which the DHTF results may be considered reliable are pertinent to the following two problems, among others:

(1) Current efforts at achieving thermonuclear reactions are aimed at producing temperatures well above 100 volts in deuterium at gaseous densities. Since both high temperature and low density reduce the importance of electrostatic interactions between the nuclei and electrons, it is evident from Figure 1 that electrostatic effects are completely negligible under the above conditions.

(2) In the early years of the Debye-Hückel theory, several attempts were made to apply the theory (primarily in its linearized form and using Boltzmann statistics for all particles) to the problem of ionized material in stellar interiors. Thus for iron at a density 156 g/cc and a temperature of $26.36 \cdot 10^6$°K (kT = 2271 ev), Fowler and Guggenheim[13] calculated the electrostatic effects to reduce the pressure by 21.9%, while Eddington[14] corrected the theory in some respects and found an effect of only 6.8%. The present DHTF theory gives for iron under these conditions pv/kT = 24.0, and thus a pressure only 4% less than the perfect-gas value for the 24-fold ionized atoms assumed by Eddington.

B. Radial Distribution Functions

In Figures 5 and 6 are shown the radial distribution functions (5), (24), and (26) for iron at normal density, $\lambda = 1$, and kT = 100 and 1000 ev.

For small r, the density of electrons about a nucleus (n_{-+}) becomes infinite as $r^{-3/2}$, just as in the Thomas-Fermi theory of the atom. As a result of the high electron density near a nucleus (of not-too-low Z), the distribution of electrons about a typical electron (n_{--}) shows a maximum

for relatively small r, and at some larger r, n_{--} even becomes greater than n_{+-}. This behavior is particularly pronounced for low temperature and density and for high Z. For Z = 1, no maximum in n_{--} has been observed; this is to be expected since in this case, there is only one electron per nucleus and consequently no strong bunching of several electrons about each nucleus.

The distribution of nuclei about a given nucleus (n_{++}) is shown in greater detail in Figures 7 to 9, which correspond to the cases pictured in Figures 2 to 4, respectively. For a given density, the effect of an increase in temperature is qualitatively what one would expect -- an increase in n_{++} at small r and a decrease at large r. However, at low density (Figure 9), the effect is quantitatively abnormal; on the scale of the figure, the only perceptible change in n_{++} on increasing kT from 10 to 100 ev is a decrease everywhere. This behavior is more pronounced the lower the density and the higher the value of Z. It is closely related to the fact that in the zero-temperature limit, n_{++} tends to a step function with the step at a radius r_1 which is less than r_o -- this last being the radius of a sphere whose volume is the average volume per atom ($4\pi r_o^3/3 = n_{+o}^{-1}$).

The reason why r_1 is less than r_o is easily seen. At zero temperature, the normalization condition (19), (20) reduces to

$$Z = 4\pi \int_o^{r_1} n_{-+} r^2 dr.$$

Since n_{-+} is everywhere greater than the average value n_{-o}, it follows that the volume inside r_1 must be less than the average volume per atom and hence $r_1 < r_o$. Indeed, at T = 0, the differential equation (16) and boundary

conditions (17) reduce precisely to the Thomas-Fermi equations for an atom of radius r_1.[5] In the case of iron with r_o corresponding to ten times normal density, the TF pressure for an atom of radius r_1 is about five times that for radius r_o.[1] The fact that the DHTF pressure is only forty percent greater than the TF value (low-temperature portion of Figure 7) shows that the DHTF theory compensates in large degree for the small value of r_1. Nonetheless, it is felt that the DHTF results should be viewed with reservations up to temperatures at which the distribution function $n_{++}(r)$ begins to exhibit some semblance of symmetry about the point $r = r_o$.

C. Energy

In Figure 10, the energy difference $E(T,\rho) - E(T=0,\rho_o)$ (where ρ_o is the normal density of the material) is plotted against T for normal density iron, for both the DHTF and TF theories. The curves are similar to those of Figure 3 for the pressure -- at high temperatures the DHTF curve lies close to the TF one, but at low temperatures, the DHTF curve may lie as much as a factor two above the other.

Rough values of the binding energy of some atoms are given in Table I. It may be seen that (except at low Z) the DHTF theory gives even greater values for $\left|E(T=0\ ,\ \rho_{p=0})\right|$ than does the TFD theory. This may be partly due to the correlation energy, which at low densities is greater (in magnitude) than the exchange energy of the TFD theory;[4] probably it is also partly the result of the contraction of the electrons around a nucleus (the fact that $r_1 < r_o$, discussed above).

It may be noted that whereas the TFD theory gives greater binding and lower specific heat than the TF theory,[2] the DHTF theory gives about the same or even greater binding than the TFD theory but apparently a higher specific heat than the TF theory.

It should perhaps be pointed out that the DHTF theory as presented in Section 2 is inconsistent in that the electron correlation energy is not included in the exponent of the energy-distribution functions used in calculating the electron densities, Eqs. (6), (24), and (26). It is also thermodynamically inconsistent in the manner of all non-linearized Debye-Hückel theories,[15] but these points will not be considered in this paper.

Table I. Atomic binding energy, E(T=0,p=0), ev/atom

Z	TF[a]	TFD[a]	DHTF
1	-20.91	-28.07	-26.3
6	-1368	-1492	-1475
26	-41885	-43280	-43590
92	-799150	-810500	-824000

[a]Reference 2.

FOOTNOTES

[1]R. Latter, Phys. Rev. 99, 1854 (1955).

[2]R. D. Cowan and J. Ashkin, Phys. Rev. 105, 144 (1957).

[3]R. J. Plock, Thesis, Yale University, 1956; R. J. Plock and J. G. Kirkwood, to be published.

[4]R. D. Cowan and J. G. Kirkwood, to be published.

[5]See, for example, Feynman, Metropolis, and Teller, Phys. Rev. 75, 1561 (1949), Sec. V.

[6]These are the usual Thomas-Fermi units except that e has been replaced by λe.

[7]J. McDougall and E. C. Stoner, Trans. Roy. Soc. (London), 237A, 67 (1938).

[8]See, for example, A. H. Wilson, Thermodynamics and Statistical Mechanics (Cambridge Univ. Press, 1957), Sec. 6.3.

[9]See, for example, Hirschfelder, Curtiss, and Bird, Molecular Theory of Gases and Liquids (John Wiley & Sons, Inc., New York, 1954), Secs. 3.1b and 6.2b.

[10]This result can also be obtained by a straightforward evaluation of the Coulomb integrals for $\lambda = 1$,

$$E_p = \frac{1}{2}\int (Ze)\rho_+ r^{-1}dr + \frac{1}{2} Z \int (-e)\rho_- r^{-1}dr,$$

where ρ_+ and ρ_- are defined in Eqs. (2) and (21), and the factors 1/2 must be included to avoid counting pair interactions twice.

[11]Reference 5, Sec. II.

[12]This procedure is almost essential to insure consistent values of A_e for use in evaluating the derivatives $(\partial A_e/\partial v)$ and $(\partial A_e/\partial T)$.

[13]R. H. Fowler and E. A. Guggenheim, Monthly Notices Roy. Astron. Soc. 85, 939 (1925).

[14]A. S. Eddington, Monthly Notices Roy. Astron. Soc. 86, 2 (1926).

[15]R. H. Fowler and E. A. Guggenheim, Statistical Thermodynamics (Cambridge Univ. Press, 1956), Chap. IX (especially §923).

FIGURE CAPTIONS

Fig. 1. Variation of pressure with temperature according to the DHTF and TF theories of the atom for deuterium at normal liquid density, $\rho = 0.17$ g/cc (or for hydrogen at $\rho = 0.085$ g/cc). p_i is the pressure of a mixture of uncharged (Boltzmann) nuclei and (quantum-degenerate) electrons.

Fig. 2. Variation of pressure with temperature for iron at ten times normal density ($\rho = 78.5$ g/cc).

Fig. 3. Variation of pressure with temperature for iron at normal solid density ($\rho = 7.85$ g/cc).

Fig. 4. Variation of pressure with temperature for iron at one-tenth normal density ($\rho = 0.785$ g/cc).

Fig. 5. The radial distribution functions for iron at normal density, $\lambda = 1$, and $kT = 100$ ev.

Fig. 6. The radial distribution functions for iron at normal density, $\lambda = 1$, and $kT = 1000$ ev. The n_{--} curve lies above the n_{-+} curve for $r/r_o > 0.892$.

Fig. 7. The distribution of nuclei about a given nucleus for iron at ten times normal density and $\lambda = 1$.

Fig. 8. The distribution of nuclei about a given nucleus for iron at normal solid density and $\lambda = 1$.

Fig. 9. The distribution of nuclei about a given nucleus for iron at one-tenth normal density and $\lambda = 1$.

Fig. 10. Temperature dependence of energy for iron at normal density ($\rho = 7.85$ g/cc). The dotted curve is for a mixture of nuclei and electrons without electrostatic interactions.

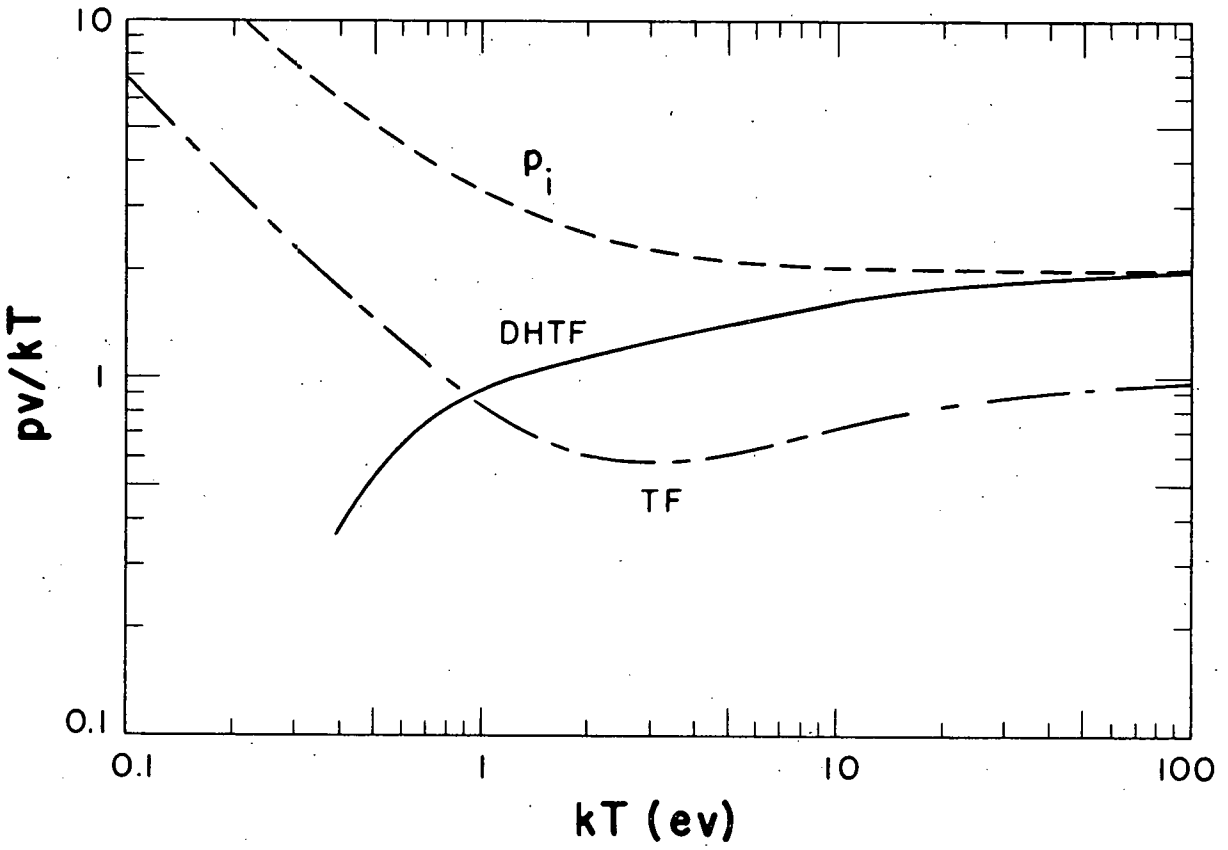

Fig. 1

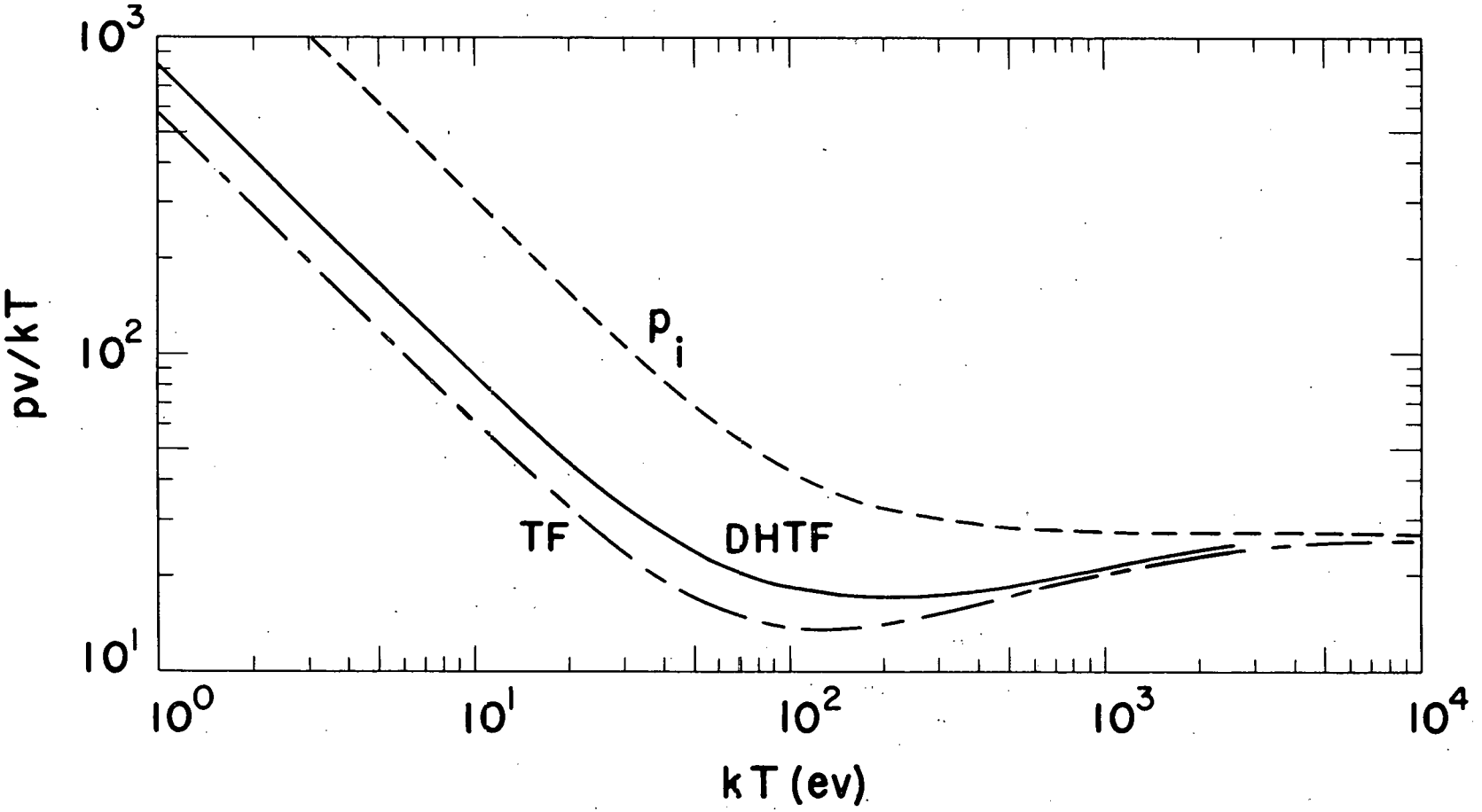

Fig. 2

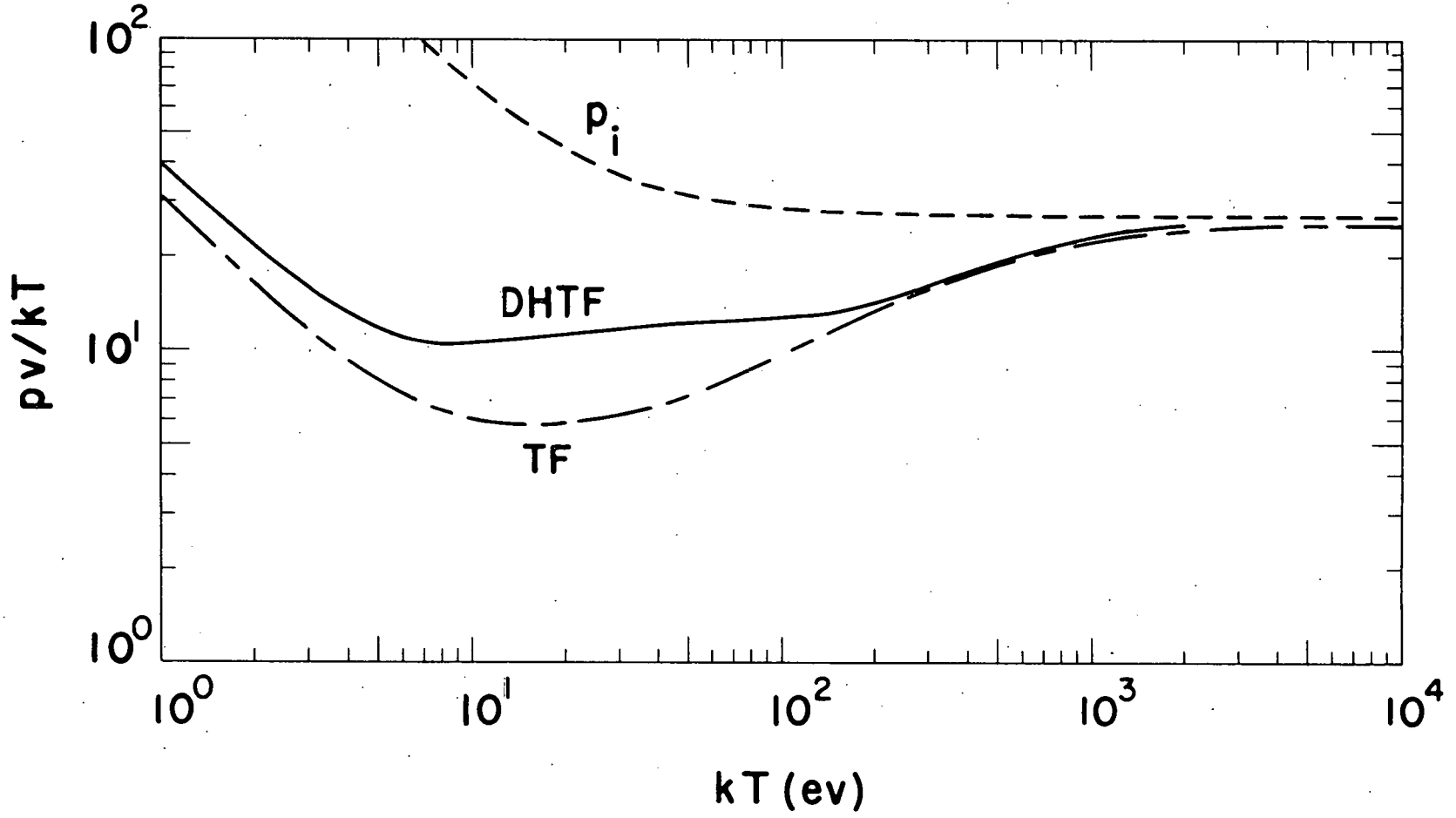

Fig. 3

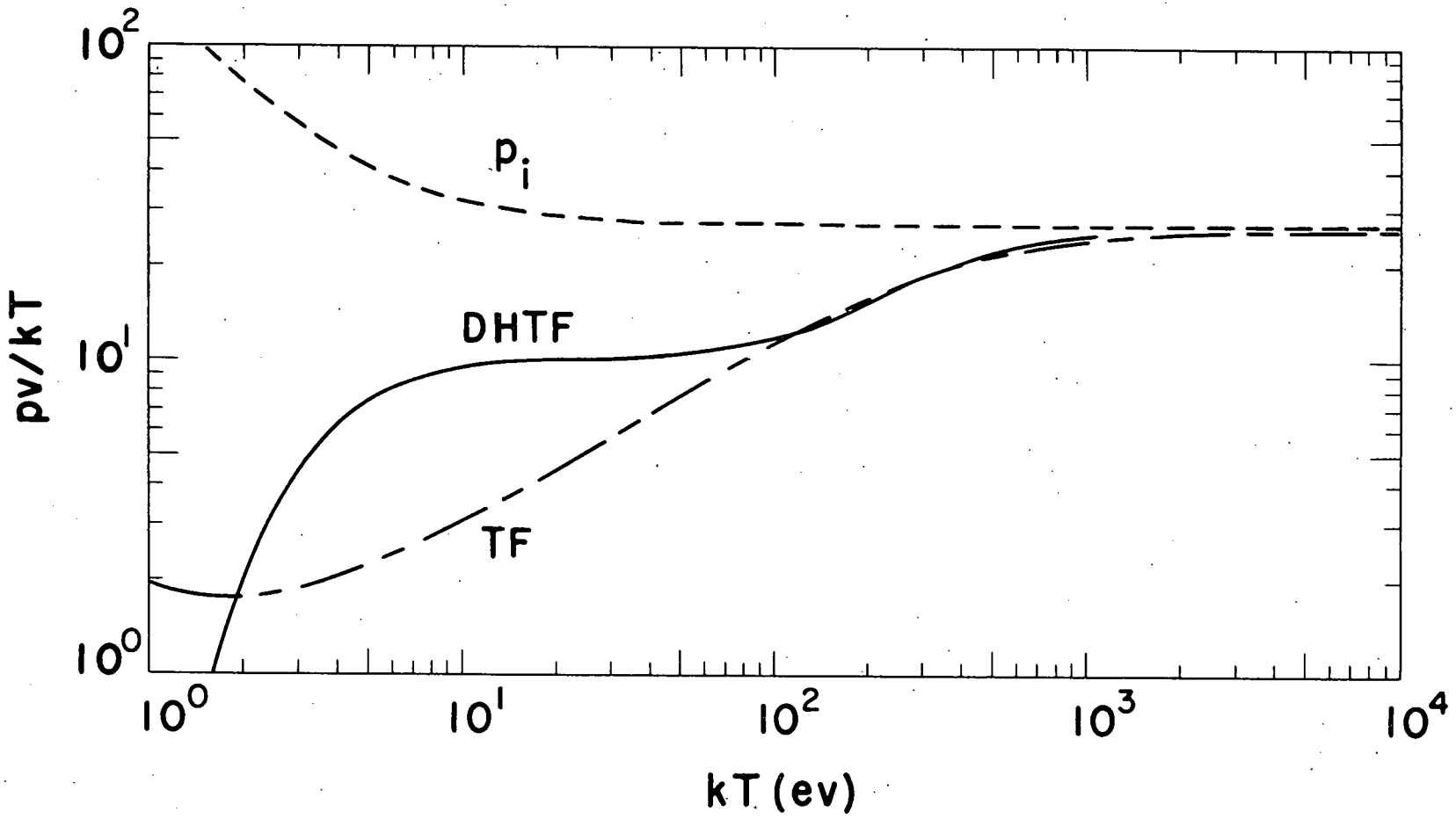

Fig. 4

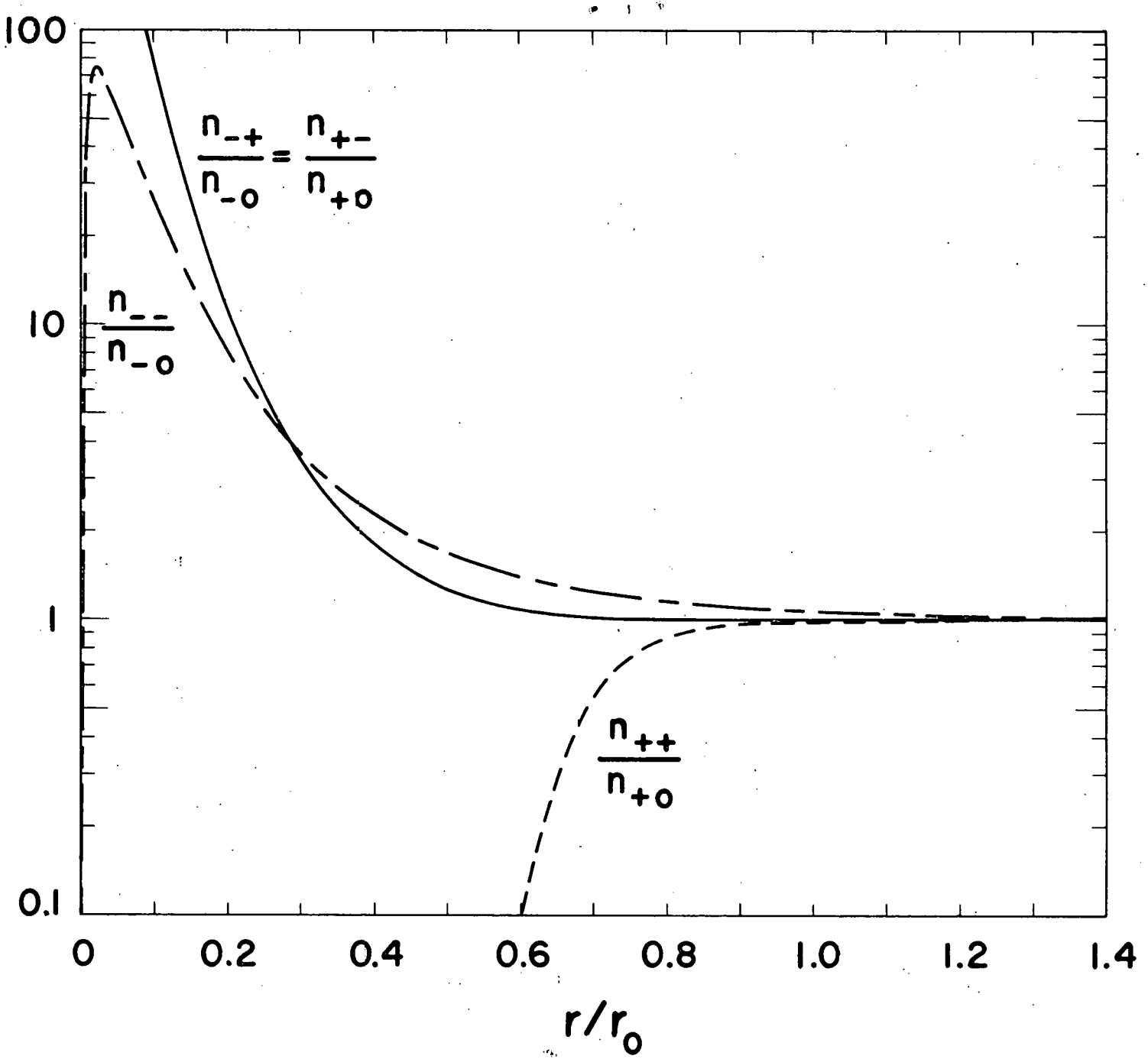
100
10
1
0.1
$\frac{n_{-+}}{n_{-o}} = \frac{n_{+-}}{n_{+o}}$
$\frac{n_{--}}{n_{-o}}$
$\frac{n_{++}}{n_{+o}}$
0
0.2
0.4
0.6
0.8
1.0
1.2
1.4
r/r_o

Fig. 5

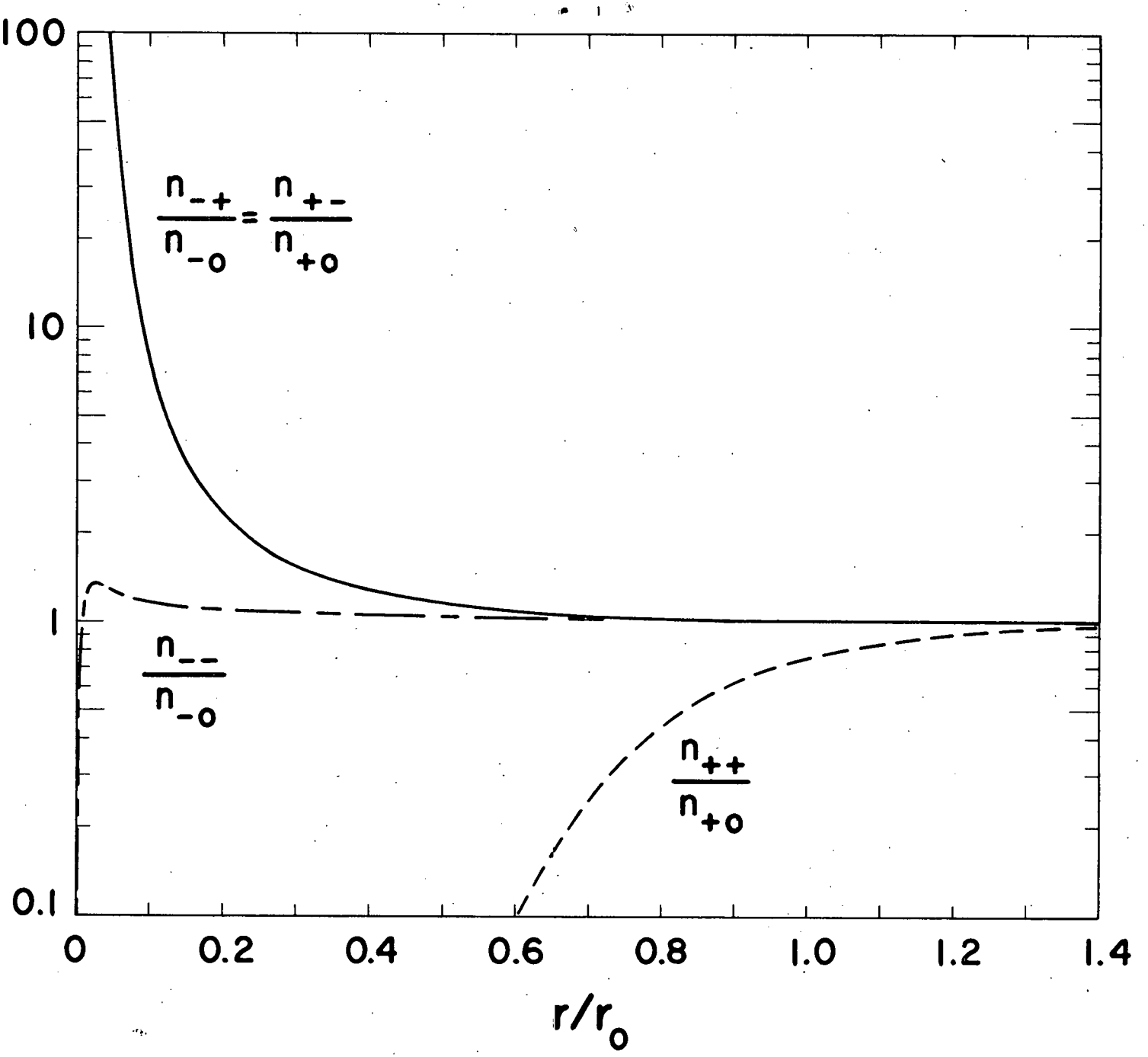

Fig. 6

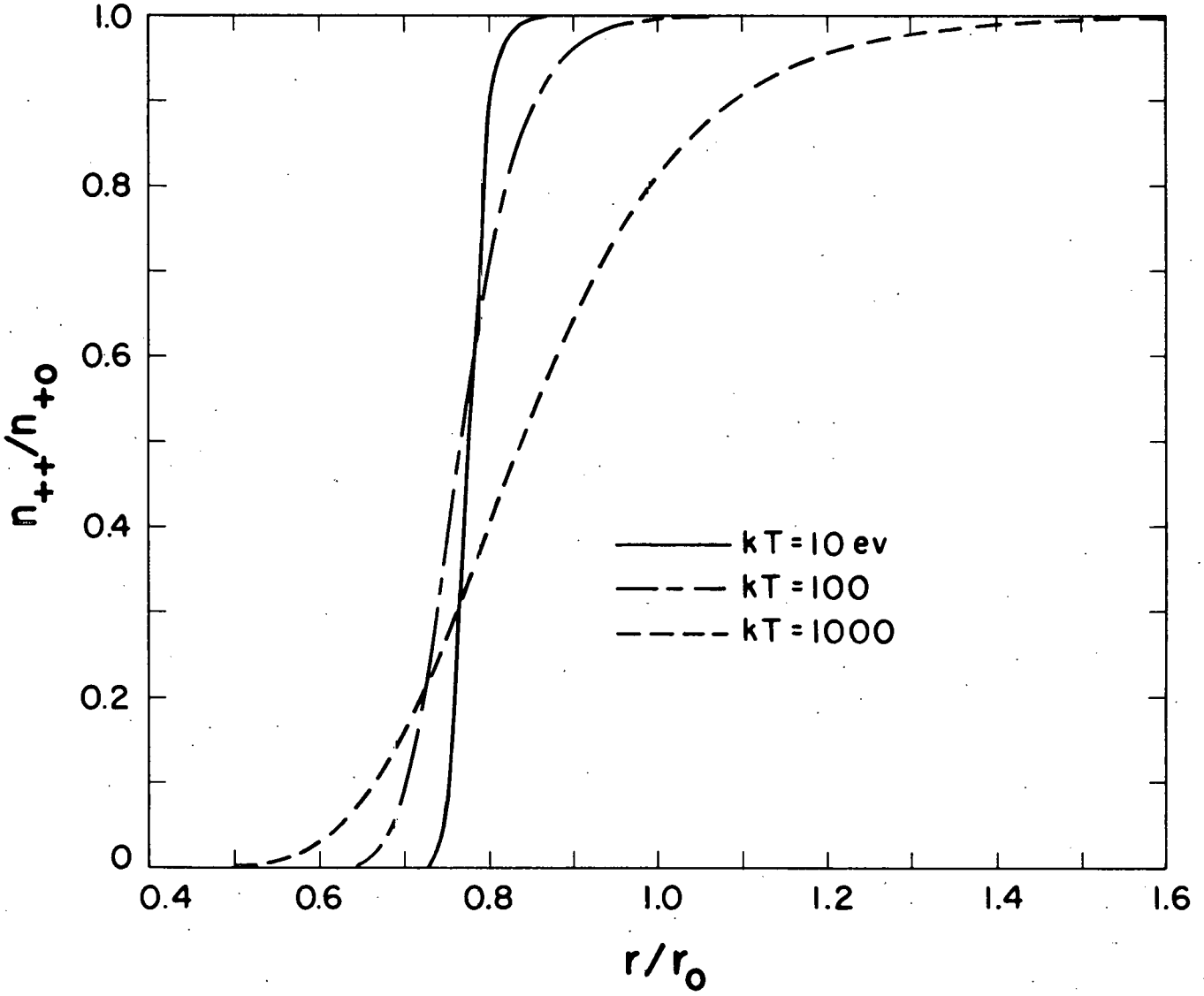

Fig. 7

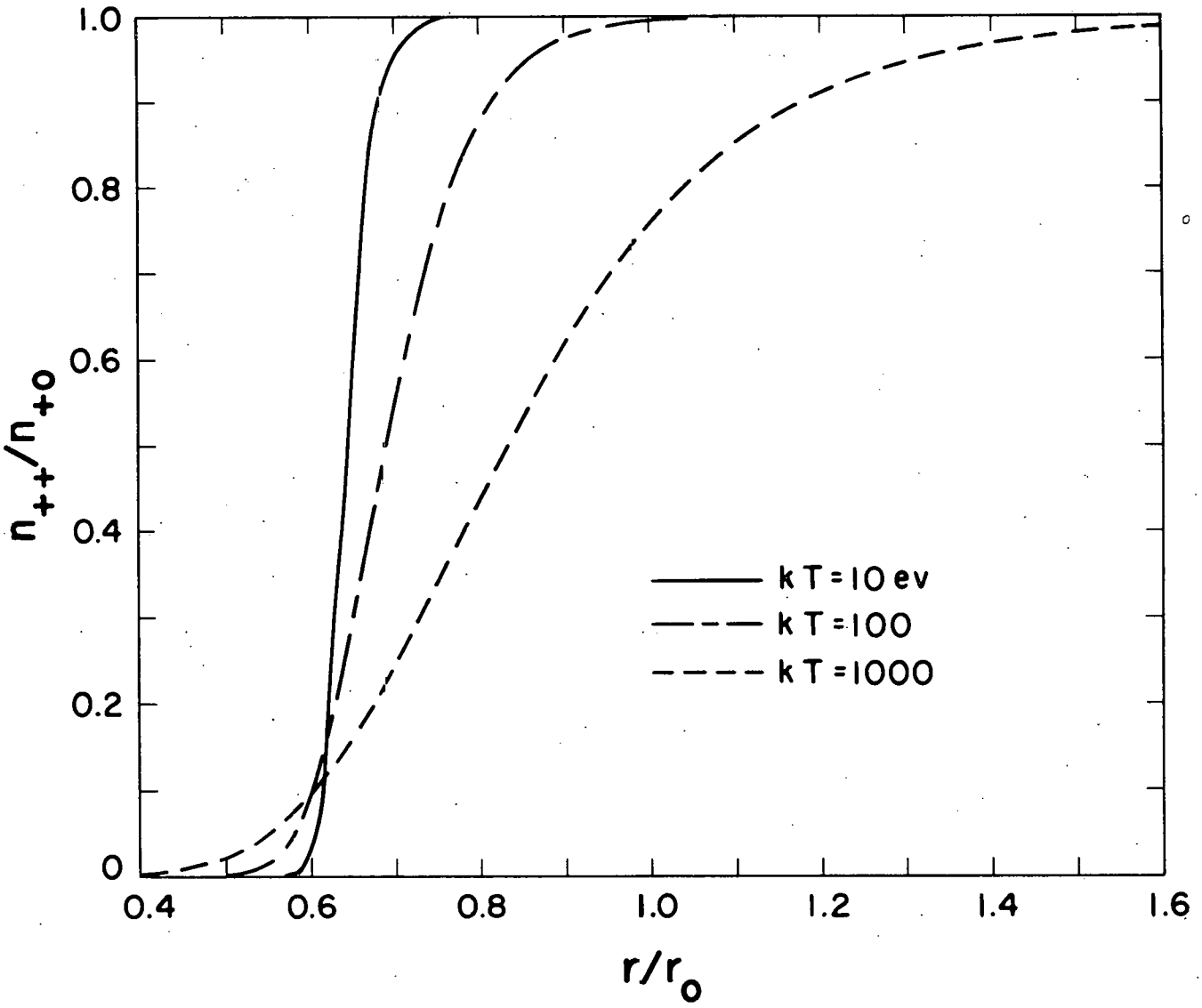

Fig. 8

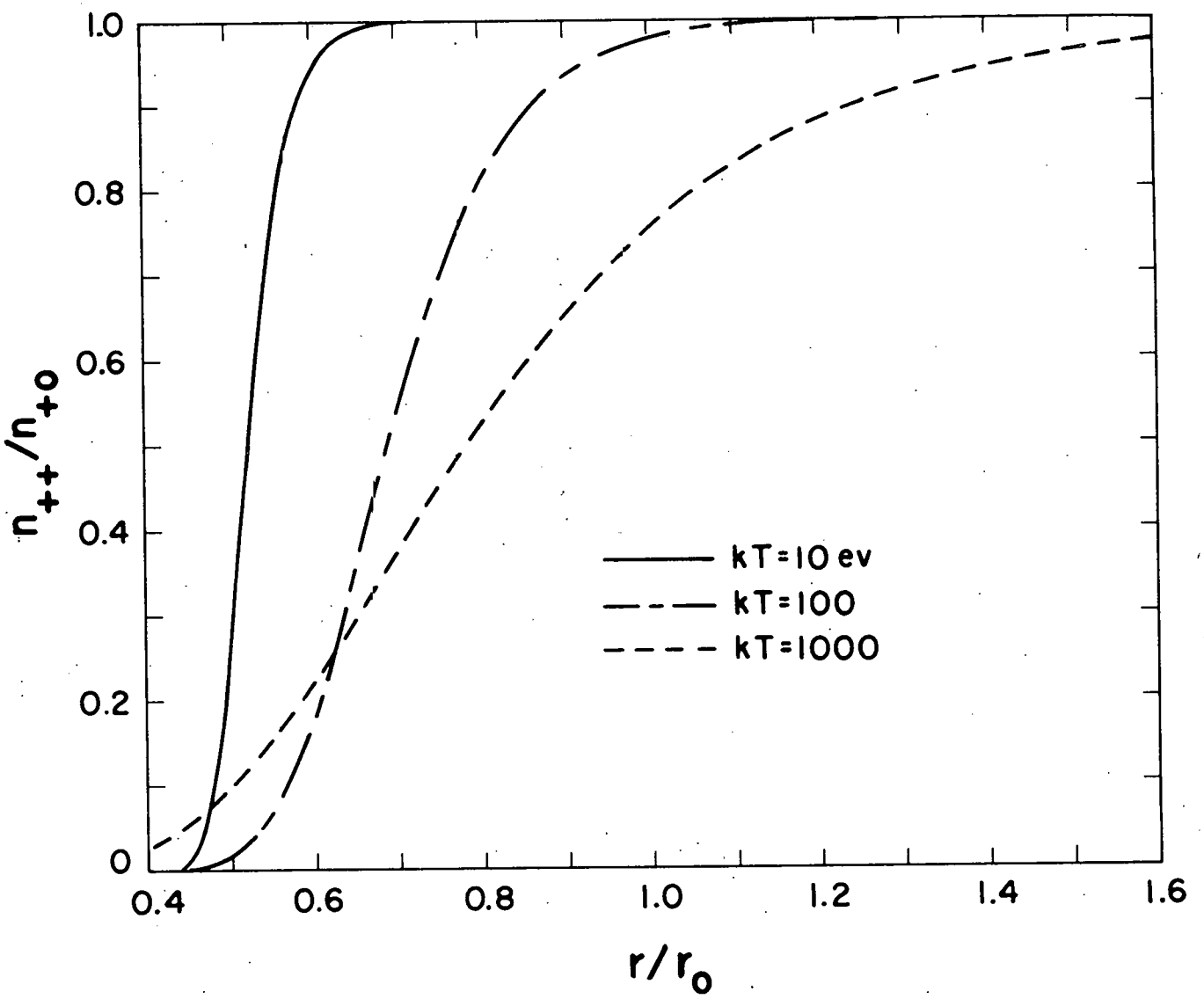

Fig. 9

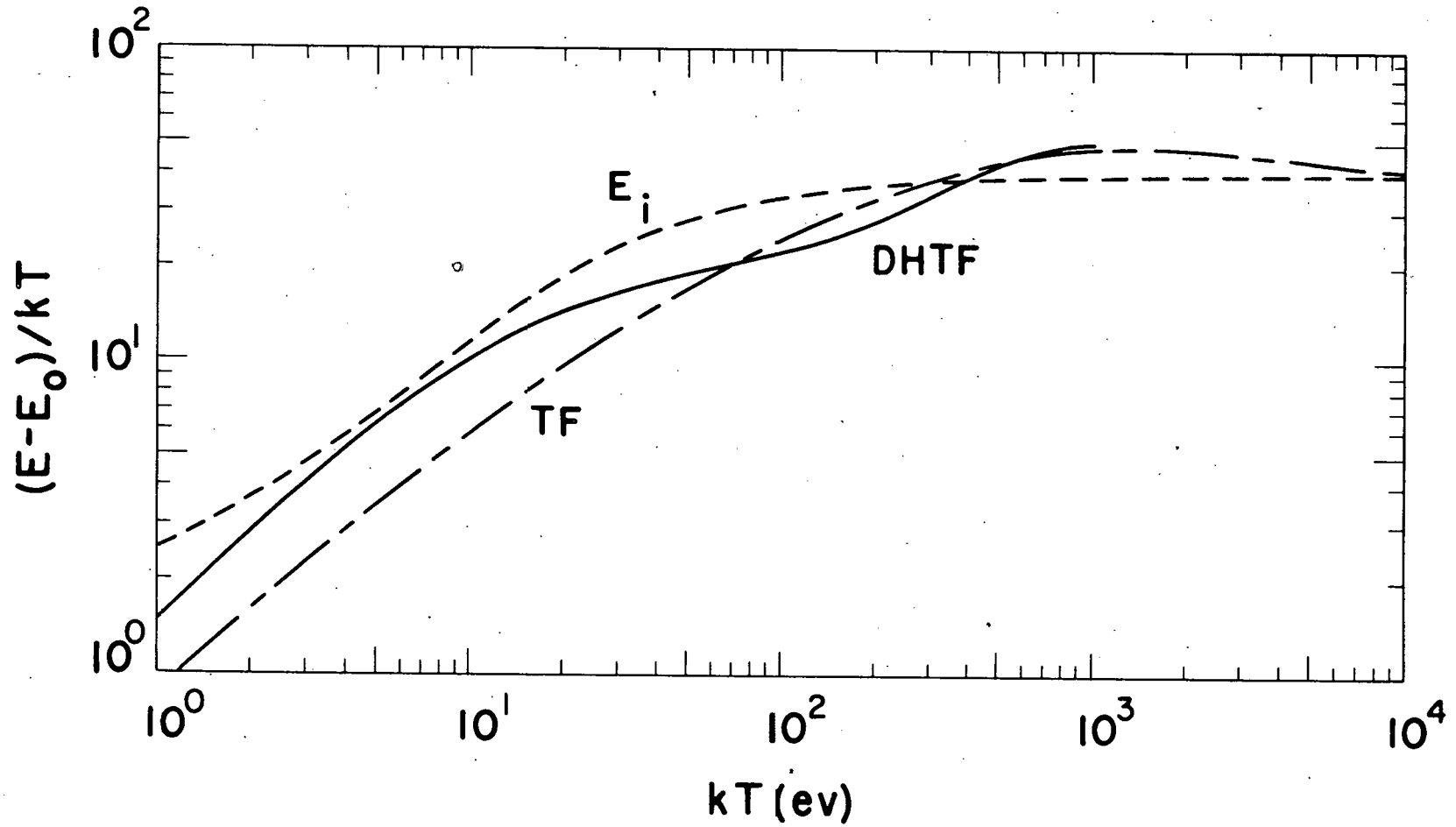

Fig. 10